Electrical resistance and magnetic properties of the neptunium monopnictides NpAs, NpSb, and NpBi at high pressures

V. Ichas and S. Zwirner
European Commission, Joint Research Centre, Institute for Transuranium Elements, Postfach 2340, D-76125 Karlsruhe, Germany

D. Braithwaite
Département de Recherche Fondamentale sur la Matière Condensée, SPSMS/LCP, CEA/Grenoble, 17 Rue des Martyrs, 38054 Grenoble Cedex 9, France

J. C. Spirlet and J. Rebizant
European Commission, Joint Research Centre, Institute for Transuranium Elements, Postfach 2340, D-76125 Karlsruhe, Germany

W. Potzel
Physik Department E-15, Technische Universität München, D-85747 Garching, Germany
(Received 26 February 1997)

We report on high-pressure studies performed on the neptunium pnictides NpAs and NpBi via electrical resistance up to ~25 GPa between 1.3 K and room temperature, and on a high-pressure investigation up to 9 GPa and at 4.2 K on NpSb using ^{237}Np Mössbauer spectroscopy. This work extends previous high-pressure studies carried out on NpAs via Mössbauer spectroscopy, on NpSb via resistance, and on all pnictides via x-ray study. In NpX (X=As,Sb,Bi) crystallizing in the cubic-NaCl phase the ground state is antiferromagnetic and displays a noncollinear 3**k** spin structure. The strong increase of the resistivity with decreasing temperature observed in the temperature range of the 3**k** order at ambient pressure collapses at 0.23 (NpAs), 2.7 (NpSb), and 3.9 GPa (NpBi). No significant change of the hyperfine interactions is found in NpAs or NpSb at the pressure where the resistance collapse is observed. The Kondo anomaly of the resistivity observed at ambient pressure disappears above 25 GPa (NpAs), 2.7 GPa (NpSb), and 3 GPa (NpBi). The Néel temperature T_N of all compounds and the ordered moment of NpAs and NpSb decrease with reduced volume. For NpAs and NpBi the resistance indicates the presence of magnetic order at least up to 16 GPa. The compounds undergo a pressure-induced structural transition with a volume reduction by ~10%. Although in the resistance of NpSb the signature of magnetic order is lost already at 8 GPa in the high-pressure phase, a magnetic hyperfine field is present, which is reduced by ~30% relative to the NaCl phase. It is suggested that the resistance collapse is caused by a change of the magnetic structure, that the decrease of T_N is due to a modification of the Fermi surface besides a small $5f$ delocalization, and that in NpSb the volume reduction in the structural high-pressure phase leads to an enhanced $5f$ delocalization. [S0163-1829(97)03241-4]

I. INTRODUCTION

The intermetallics of Ce and the light actinides U and Np exhibit a broad range of electronic and magnetic behavior, since in contrast to the classical rare-earth systems the $4f$ (Ce) and $5f$ electrons (U, Np) hybridize with the conduction band. This leads in most cases to a partial quenching of the ordered magnetic moment via $5f$ delocalization, Kondo compensation, or crystal-field splitting. The Kondo compensation is caused by the antiferromagnetic exchange between the f states and the conduction band driven by hybridization.[1] This often leads to an anomaly of the electrical resistivity, i.e., a logarithmic decrease with rising temperature, in the paramagnetic range.[1,2]

The pnictides of neptunium NpX discussed in the present work (X=As,Sb,Bi) all crystallizing in the cubic-NaCl structure at ambient pressure behave in many respects similarly and display some remarkable properties. Their ordering temperatures 173 K (for NpAs), 200 K (NpSb), and 193.5 K (NpBi) are comparatively high.[3] Neutron and Mössbauer experiments revealed that in the ground state their ordered moment (~$2.6\mu_B$) and electric quadrupole coupling constant (−26 – −31 mm/s) at the Np nucleus are close to the theoretical value expected for a Np^{3+} free-ion state ($2.57\mu_B$ and −27 mm/s, respectively).[4–8] This seems to suggest that the effects of crystal-field splitting, $5f$ hybridization, or Kondo compensation are relatively small, although a considerable $5f$-ligand p mixing is expected.[9] The three systems are characterized as semimetals due to their low carrier density as deduced from Hall-effect measurements[3,10,11] and their high values of the room-temperature resistivity, larger than 1 mΩ cm. Interestingly a resistivity Kondo anomaly is observed in the paramagnetic range.

The three systems displays an antiferromagnetic ground state with a noncollinear 3**k** structure.[4–6] Multi-**k** structures are rarely found in systems where no $4f$ or $5f$ electrons are involved. They appear rather frequently in actinide compounds.[12] It has been shown for NpAs that the onset of the 3**k** structure is accompanied by a lattice expansion of ~0.4%.[13] As in some other pnictides, e.g., CeP,[14] CeAs,[15] USb,[16] the onset of the 3**k** structure coincides with a sharp upturn of the resistivity, which can be explained by a de-

crease of the carrier density due to a change of the Fermi surface.[3,9]

In the Ce and U pnictides mentioned above the resistivity goes through a maximum below the transition temperature $T_{3\mathbf{k}}$ of the 3**k** structure and then decreases at 4.2 K to a value below the room-temperature value. In contrast, in NpSb and NpBi the resistivity displays no maximum and increases instead drastically to more than 40 Ω cm and 150 mΩ cm, respectively, at 1.3 K, resembling a semiconducting behavior. The case of NpAs is intermediate, $\rho(T)$ displays a maximum below $T_{3\mathbf{k}}$ but the low-temperature value is about twice as large as ρ(300 K).

Recent high-pressure resistance measurements on NpSb revealed that the sharp upturn of ρ at $T_{3\mathbf{k}}$ disappears above 2.3 GPa.[17] This was taken as a hint for the disappearance of the 3**k** phase. Furthermore, between ambient pressure and 2.3 GPa $T_{3\mathbf{k}}$ decreases strongly with reduced volume ($d \ln T_{3\mathbf{k}}/-d \ln V=-3.1$). The Kondo anomaly in the paramagnetic range disappears above 2.7 GPa.

Pressure is an elegant way to tune certain model parameters, e.g., the exchange interaction or the magnetic moment, which allows one to compare their volume dependencies with what is expected from predictions of theory or phenomenology in actinide research. From previous Mössbauer effect measurements on NpAs the 3**k** phase was suggested to persist in the ground state up to ~2.5 GPa and to coexist with a collinear $4\uparrow4\downarrow$ structure at higher pressures.[18,8] Furthermore, the ordering temperature of NpAs decreases more slowly than in NpSb. It was proposed that the stronger decrease of T_N in NpSb is connected with a considerable $5f$ hybridization with reduced volume, which may lead to a strong reduction of the magnetic moment.

Previous x-ray measurements revealed that all the three compounds NpX undergo structural phase transformations at 25–40, 10–18, and 8.5 GPa, respectively.[19] The previous resistance results on NpSb seemed to indicate that magnetic order disappears in the high-pressure phase and that the $5f$ electrons strongly delocalize.[17]

To extend the previous high-pressure work on NpX and to examine some of the suggestions described above we performed high-pressure resistance measurements on NpAs and NpBi up to ~25 GPa and Mössbauer measurements on NpSb up to 9 GPa. This allows us to investigate three important aspects, the changes of the magnetic phases, particularly the 3**k** phase, the influence of the structural transition on $5f$ delocalization, and the magnetic behavior in terms of $5f$ delocalization in the NaCl phase.

II. EXPERIMENT

In the resistance experiments thin platelets of NpAs and NpBi of dimensions approximately $0.6\times0.2\times0.03$ mm^3 were cleaved from a larger single crystal, the growth of which has been described elsewhere.[20] The electrical resistance of the sample placed inside of a sintered diamond-anvil device was determined by the four-probe method. We used steatite as pressure transmitting medium providing quasi hydrostatic conditions. Successive cooling and heating cycles from 300 K down to 1.5 K were performed up to 25 GPa. The pressure was determined *in situ* from the superconducting transition temperature of a thin Pb foil[21] embedded with the sample.

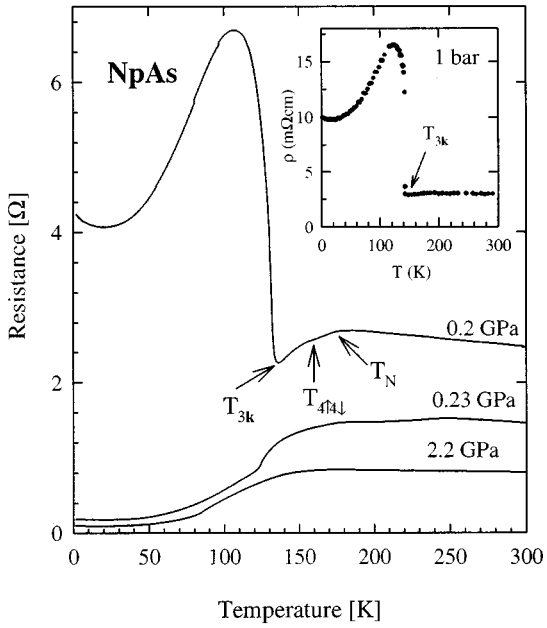

FIG. 1. NpAs: Resistance vs temperature curves at low pressures. The resistivity curve at ambient pressure taken from Refs. 11 and 3 is shown in the inset. The arrows point to the magnetic transitions extrapolated from the ambient pressure result. T_N is the Néel temperature, $T_{4\uparrow4\downarrow}$ corresponds to the transition from the incommensurate to the commensurate $4\uparrow4\downarrow$ structure, and $T_{3\mathbf{k}}$ indicates the onset to the triple k structure.

Mössbauer transmission experiments on the 60 keV γ rays of ^{237}Np were carried out using a ^{241}Am metal source (about 50 mCi). The absorber was a powder sample crushed from a single crystal of NpSb. The powder was compressed into a pellet of 4.5 mm diameter and 0.2 mm height with a thickness of ~100 mg/cm^2 of ^{237}Np, and encapsulated in Al for radiation safety. The Al capsule (5 mm diameter, 0.7 mm height, 0.25 mm wall thickness) was mounted inside a high-pressure cell of the Bridgman type using B_4C anvils. The Al capsule and a small amount of paraffin between the capsule and the anvils served as pressure transmitting media. The rather large absorber area restricted the pressure range to ~9 GPa. The pressure was determined with a Pb manometer similar to the resistance experiment. Details of the Mössbauer high-pressure spectrometer can be found in Ref. 22.

III. RESULTS

A. Resistance of NpX (X=As,Bi) and comparison to NpSb

Since the sample geometry is not precisely known, we use the resistance R rather than the specific resistivity ρ to present the data. The detailed resistance study of NpSb under pressure has been published in Ref. 17. In order to give a better overview we compare our new results on NpAs and NpBi with the data obtained previously for NpSb. The resistance versus temperature curves under pressure are shown in Figs. 1–3 for NpAs, in Fig. 4 for NpSb, and in Figs. 5 and 6 for NpBi.

The ambient pressure resistivities are plotted in the insets of Figs. 1,[11,3] 4,[23] and 5,[3,10] respectively. For all compounds,

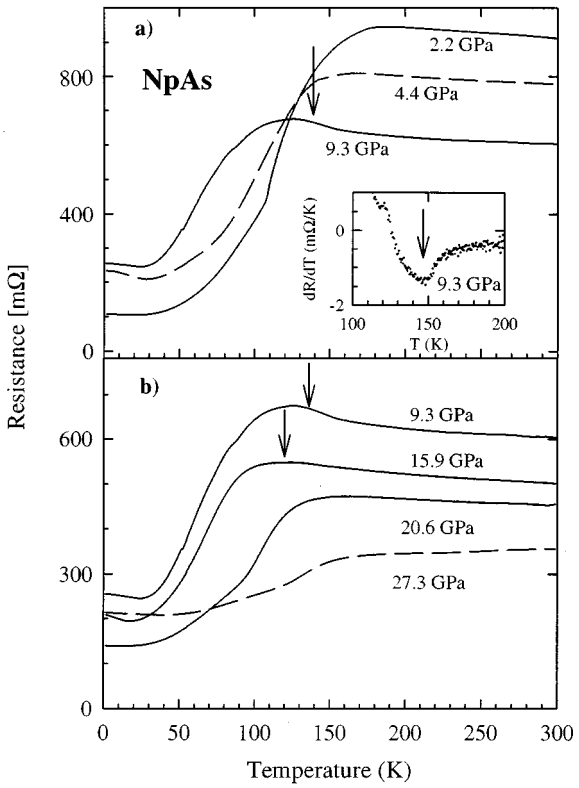

FIG. 2. NpAs: Resistance vs temperature curves (a) from 2.2 up to 9.3 GPa, (b) from 9.3 up to 27.3 GPa. The arrows indicate the presumed magnetic order. The corresponding ordering temperature is extracted from the derivative dR/dT as shown for one pressure in the inset of (a).

the high values of the resistivity ρ at 1 bar and in the paramagnetic range ($\geqslant 1$ mΩ cm) have been attributed to a semimetallic behavior.[3] Furthermore, a strong increase of ρ appears at the onset of the $3\mathbf{k}$ magnetic structure (at $T_{3\mathbf{k}}$ $=140$, 200, and 193.5 K, respectively) which in the case of NpSb and NpBi even resembles a semiconducting behavior. In NpAs, a collinear $4\uparrow 4\downarrow$ and an incommensurate magnetic

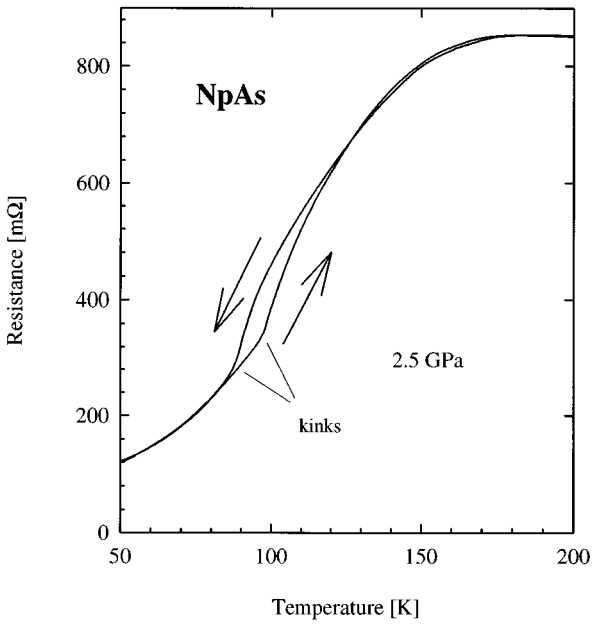

FIG. 3. NpAs: Hysteresis behavior of the kinks in the resistance vs temperature curve at 2.5 GPa (see Secs. III A and IV A).

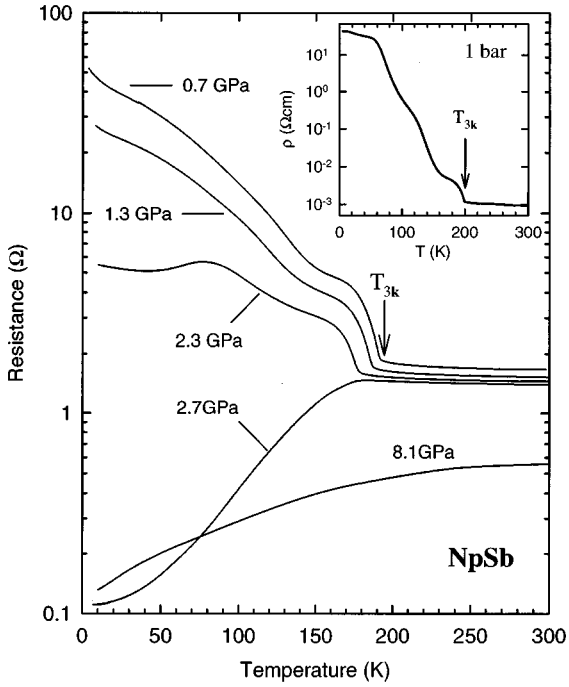

FIG. 4. NpSb: Resistance shown in logarithmic scale vs temperature at different pressures. The data are taken from Ref. 17. The inset shows the ambient pressure resistivity (Ref. 23). The arrow points to the onset of magnetic order.

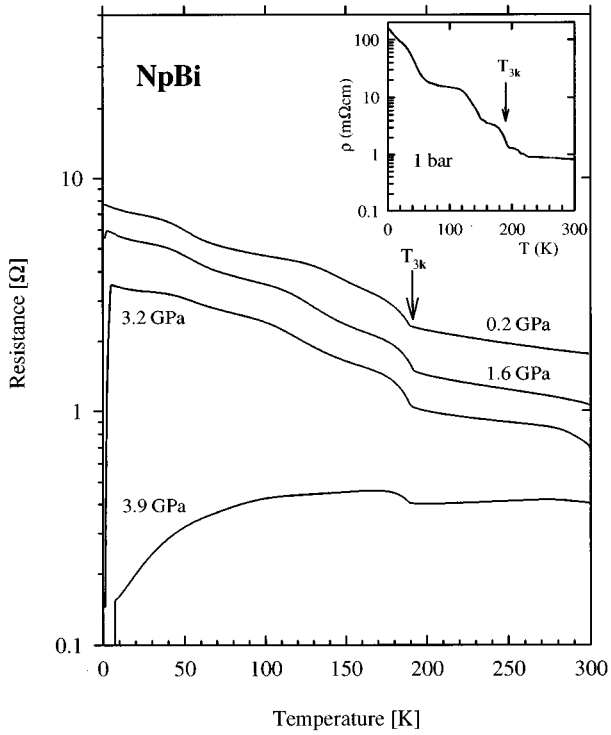

FIG. 5. NpBi: Resistance shown in logarithmic scale vs temperature at pressures up to 3.9 GPa. The inset displays the ambient pressure resistivity taken from Refs. 10 and 3. The arrows show the onset of magnetic order.

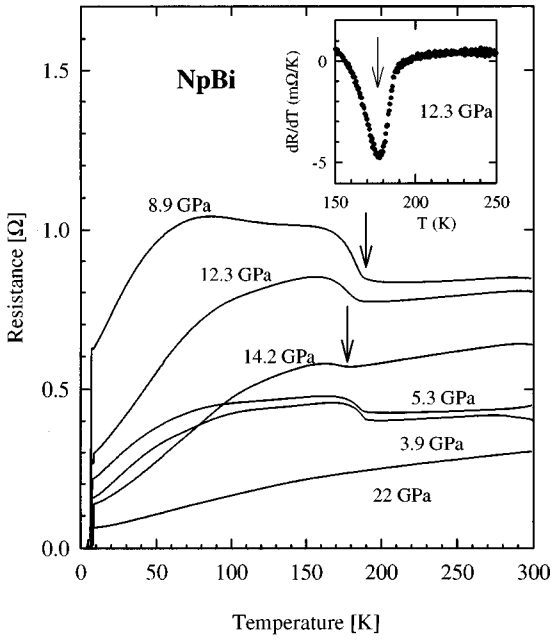

FIG. 6. NpBi: Resistance vs temperature curves between 3.9 and 22 GPa. The arrows point at the signature of magnetic order at high pressures. The corresponding ordering temperatures are extracted from the derivative dR/dT as shown in the inset for one pressure. The superconducting transition above 3.9 GPa and below 10 K is due to traces of bismuth in the NpBi sample (see text).

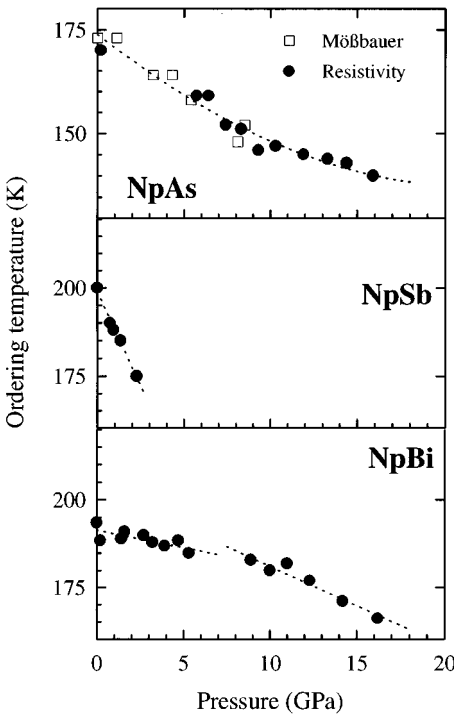

FIG. 7. Pressure variation of the Néel temperature T_N obtained from our resistance data (●) for NpAs, NpSb (Ref. 17), and NpBi and from Mössbauer data (□) for NpAs (Ref. 18).

structure are present above 140 K.[4] They are visible as two small anomalies at $T_{4\uparrow 4\downarrow}=156$ K and $T_N=173$ K. In the paramagnetic range, a logarithmic variation of the resistance is present in all compounds which is typical for a Kondo behavior.

First we compare our results at the lowest pressures investigated with the previous measurements at 1 bar. All essential qualitative features described above are also present at 0.2 GPa (NpAs), 0.7 GPa (NpSb), and 0.2 GPa (NpBi). However, we observe already considerable quantitative changes. The ratios $R_{4.2\,\mathrm{K}}/R_{300\,\mathrm{K}}$ are drastically reduced in all compounds. An estimation of the specific resistivity ρ from the resistance R shows that in the paramagnetic range the low- and ambient pressure resistivity values agree well. Consequently, the resistivity at 4.2 K is reduced by a factor of ~ 2 in NpAs, ~ 300 in NpSb, and ~ 50 in NpBi. The sharp upturn corresponding to the onset of the $3\mathbf{k}$ magnetic structure occurs at lower temperatures, 136 K in NpAs, 190 K for NpSb, and 188.5 K for NpBi, i.e., $T_{3\mathbf{k}}$ decreases under pressure. In NpAs the maximum of the resistance in the $3\mathbf{k}$ phase appears at 107 K in comparison to 123 K at ambient pressure. Furthermore, the Néel temperature slightly decreases ($T_N \approx 170$ K), whereas $T_{4\uparrow 4\downarrow}$ remains unchanged within the experimental resolution.

As pressure is increased, in all compounds a collapse of the low-temperature resistance is observed. This occurs at 0.23 GPa for NpAs (Fig. 1), 2.7 GPa for NpSb (Fig. 4), and 3.9 GPa for NpBi (Fig. 5). In NpAs and NpSb, this effect is even accompanied by a suppression of the signature of the $3\mathbf{k}$ magnetic order, i.e., the sharp upturn of the resistance. Instead, in NpAs a kink appears at ~ 120 K, i.e., between the low-temperature regime ($T<120$ K) displaying a positive curvature of $R(T)$ and the high-temperature range (120 K $<T<150$ K) showing a negative curvature. At several pressures the kink exhibits a strong hysteresis (of up to 18 K) upon decreasing and increasing temperature as shown in Fig. 3 for 2.5 GPa (see Sec. IV A). The temperature of the kink decreases with increasing pressure and the kink disappears above 3 GPa. In NpSb the upturn is replaced by a sharp decrease of $R(T)$ below 190 K. In NpBi, this upturn is still present up to 16.2 GPa.

In NpBi, a striking feature is observed above 1 GPa and below 10 K. The resistance displays a sharp decrease with reduced temperature (Figs. 5 and 6). Above 3.2 GPa, the resistance drops to zero, i.e., we observe a superconducting transition. The variation of this transition temperature T_c is not continuous as a function of pressure. T_c oscillates between ~ 6 and ~ 9 K above 4 GPa. This variation is almost identical to the variation of T_c with pressure in the different polymorphic phases of bismuth.[24] In addition, photoemission measurements on a single crystal from the same batch revealed the presence of metallic Bi.[25] Therefore we believe that this superconducting transition is due to traces of Bi in our sample.

In Fig. 7 the Néel temperatures T_N are plotted versus pressure. T_N decreases with rising pressure in the three compounds. In NpAs, the resistance anomaly at the Néel temperature is rapidly lost under pressure (Fig. 1). At several pressures above 5.7 GPa, however, an inflection point (i.e., a minimum of dR/dT) appears in the $R(T)$ curves (see arrows in Fig. 2). These inflection points (●, see Fig. 7) coincide with the Néel temperatures derived from Mössbauer experiments (□) which were performed up to ~ 8.4 GPa.[18] Therefore we suggest that the inflection points (●) also give T_N above 8.4 GPa. We find that T_N decreases from ~ 173 K at 1

bar to 140 K at 15.9 GPa with a rate of -3.0 K/GPa at low pressures. Above 16 GPa, the minimum in the derivative is no longer present.

In NpSb, the Néel temperature was determined in the pressure range up to 2.3 GPa where the sharp increase of $R(T)$ is present. The magnetic order appears as a minimum in the curves of the derivative dR/dT.[17] T_N was found to decrease at a rate of -11.5 K/GPa (Fig. 7). Above 2.3 GPa, it is difficult to determine T_N but the decrease of R below 170 K is probably due to a magnetic transition.[17]

In NpBi the signature of magnetic order is the same at ambient and elevated pressure. We can therefore easily extract the Néel temperature from our resistance data. T_N corresponds to a sharp minimum in the curves of the derivatives dR/dT which disappears above 16 GPa (inset of Fig. 6). T_N decreases at two different rates, -1.02 K/GPa below 8.9 GPa and -2.5 K/GPa above 8.9 GPa (Fig. 7).

With further increase of pressure, the signature of magnetism disappears in NpSb above 8 GPa (Ref. 17) and in NpBi above 16 GPa (Fig. 6) and their $R(T)$ curves exhibit a metallic behavior. In contrast, in NpAs a decrease of the resistance with decreasing temperature below ~ 150 K is still present above ~ 16 GPa and may be due to magnetic order (Fig. 2).

The logarithmic Kondo anomaly found at ambient pressure in the paramagnetic range,[3] progressively disappears above 2.7 GPa in NpSb and 3 GPa in NpBi. In NpAs, however, the Kondo anomaly is present up to ~ 25 GPa and disappears at higher pressures.

In NpAs a minimum appears below 40 K at a few pressures (Fig. 2). At present the origin of the latter feature is not understood.

In NpAs and NpSb, the resistance in the paramagnetic range decreases with increasing pressure. In contrast, the resistance variation of NpBi as a function of pressure is more complicated over the whole temperature range (Fig. 6, see Sec. IV B).

B. Mössbauer spectroscopy on NpSb

Figure 8 shows Mössbauer spectra recorded at 4.2 K at selected pressures. The spectra measured between 1 bar and 4.2 GPa were fitted assuming a single Np site with a magnetic hyperfine and a collinear axially symmetric quadrupole interaction. At 7.8 GPa an additional line broadening of the outer lines was taken into account which is proportional to the magnetic splitting of the nucleus. At 9.0 GPa two subspectra were fitted (see below). The results of the measurements at 4.2 K and for all pressures investigated are summarized in Table I. The hyperfine parameters obtained at ambient pressure are in agreement with the values obtained in a previous Mössbauer study.[6] The pressure dependence of the magnetic hyperfine field B_{hf}, of the quadrupole interaction e^2qQ and of the isomer shift S is depicted in Fig. 9. The following features are observed:

Between ambient pressure and 7.8 GPa B_{hf} decreases weakly by $\sim 5\%$.

In this pressure range the coupling constant of the electric quadrupole interaction e^2qQ is nearly constant within the experimental errors. The field gradient eq is ''induced'' by magnetic order. In the NaCl structure of NpSb the Np site symmetry is cubic in the paramagnetic range, which leads to a vanishing field gradient. However, magnetic order breaks cubic symmetry at the site of the Np nuclei, i.e., a quantization axis is established, which induces a field gradient.

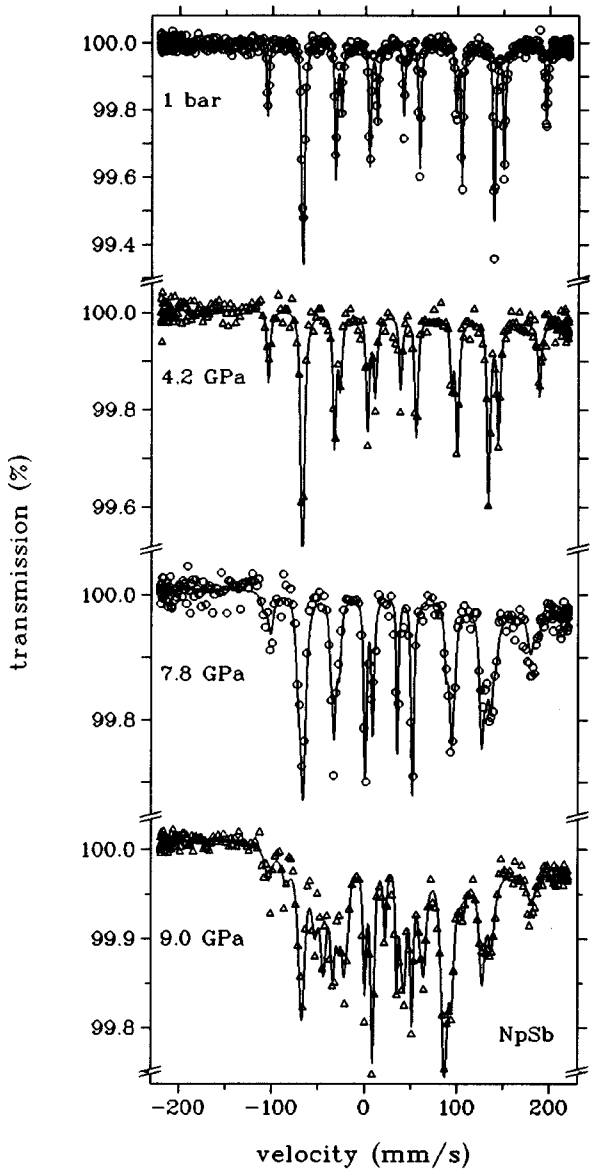

FIG. 8. NpSb: Mössbauer spectra recorded at 4.2 K and selected pressures.

The isomer shift S displays a linear decrease up to 7.8 GPa (see Fig. 9) with a normalized slope of $(1/\Delta S^{\mathrm{Np}^{3+}\rightarrow\mathrm{Np}^{4+}})\, dS/dp = 1\times 10^{-1}\ \mathrm{GPa}^{-1}$, where $\Delta S^{\mathrm{Np}^{3+}\rightarrow\mathrm{Np}^{4+}} = |S(\mathrm{Np}^{3+}) - S(\mathrm{Np}^{4+})| = 50$ mm/s is the difference in S between the Np^{3+} and Np^{4+} configurations.[26]

At 7.8 GPa fits assuming the same hyperfine pattern as at lower pressures did not show satisfactory agreement with the data, since the width of the inner lines of the spectrum are considerably smaller compared to those of the outer lines. Consequently an enhanced ratio of the amplitude of the inner to outer lines is observed. This hints to a small distribution of hyperfine fields at high pressures.

At 9.0 GPa (see Fig. 8) the hyperfine pattern displays drastic deviations in comparison to lower pressures. A careful analysis unequivocally shows that two subspectra i.e.,

TABLE I. NpSb Mössbauer results at 4.2 K for various pressures p. The magnetic hyperfine field $B_{\rm nf}$, the coupling constant of the electric quadrupole interaction e^2qQ, the isomer shift S, and the line width Γ (full width at half maximum) are listed. The isomer shift is given relative to $NpAl_2$. At 9.0 GPa the relative intensities (RI) of the subspectra due to the Np sites 1 and 2 are listed. Since the outer lines are broadened at 7.8 and 9.0 GPa, the values for the width Γ are omitted in these two cases.

p (GPa)		$B_{\rm hf}(T)$	e^2qQ (mm/s)	S (mm/s)	Γ (mm/s)	RI (%)
0.0		559(2)	−29(1)	22.5(2)	2.7(1)	
1.9(2)		552(2)	−29(1)	20.9(2)	3.8(2)	
2.7(2)		549(2)	−28(1)	20.7(2)	3.5(4)	
4.2(2)		545(2)	−29(1)	19.7(2)	4.0(4)	
7.8(3)		530(3)	−28(2)	16.8(4)		
9.0(3)	Site 1	527(4)	−28(3)	16.5(4)		52(5)
	Site 2	355(4)	+34(3)	7.4(4)		48(5)

two different Np sites are present. Site 1 can be identified with the structural and probably magnetic phase present at 7.8 GPa. At site 2, $B_{\rm hf2}$ is drastically reduced by more than 30% (see Table I), the quadrupole coupling constant $(e^2qQ)_2$ even shows opposite sign, and the isomer shift S_2 is reduced by $\sim$9 mm/s relative to S_1. The latter effect corresponds to $\Delta S/\Delta S^{Np^{3+}\rightarrow Np^{4+}}\approx 18\%$. As discussed in Sec. IV B, these striking effects are due to a sluggish structural phase transformation which was found previously.[27] The relative intensities of the two subspectra 1 and 2 are close to 1:1.

We emphasize that at 7.8 GPa our analysis excludes the onset of a structural phase transformation. A second Np site displaying strong deviations of the hyperfine interactions can be ruled out within the experimental accuracy, in contrast to the situation at 9 GPa. The line broadening is probably due to a change of the spin arrangement (see Sec. IV B).

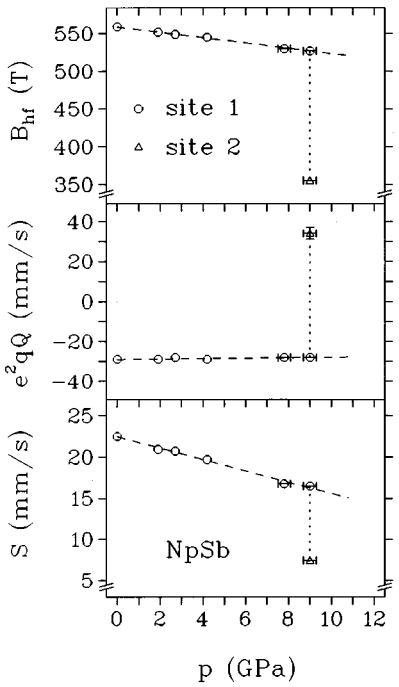

FIG. 9. NpSb: Pressure dependencies of the magnetic hyperfine field $B_{\rm hf}$, the coupling constant of the induced quadrupole interaction e^2qQ, and the isomer shift S relative to $NpAl_2$. At the highest pressure two Np sites can be distinguished, Np site 1: ○, Np site 2: △.

IV. DISCUSSION

A. Collapse of the low-temperature resistance and magnetic transformations

In the pnictides of Np the onset of the noncollinear 3**k** phase is accompanied by two features in the resistivity at ambient pressure. At the transition temperature, $T_{3\mathbf{k}}$, the resistivity displays a sharp upturn with decreasing temperature (see insets of Figs. 1, 4, and 5), which also has been observed in CeP,[14] CeAs,[15] and USb (Ref. 16) and which therefore seems to be a fingerprint of this structure.[3] In contrast to the Ce systems, in the actinide pnictides $\rho(T)$ increases far above the room-temperature values below $T_{3\mathbf{k}}$. The most remarkable pressure effect in NpAs, NpSb, and NpBi is the collapse of the low-temperature resistance which occurs at increasingly high pressures within the series (0.23 GPa for NpAs, 2.7 GPa for NpSb, and 3.9 GPa for NpBi). In NpAs and NpSb this is even accompanied by the suppression of the sharp upturn of the resistance at the onset of the 3**k** magnetic order whereas this feature is still present in NpBi up to 16.2 GPa.

For an interpretation of the resistance collapse under pressure it is crucial to understand the mechanism which gives rise to the enormous increase of the resistivity in the 3**k** phase at ambient pressure. According to Kasuya *et al.*, the onset of the 3**k** structure reduces the number of carriers at the nesting regions of the Fermi surface.[9] For this reason the carrier number and consequently the electrical conductivity is highly sensitive to the presence of the 3**k** structure. The collapse of the low-temperature resistance indicates a dramatic increase of the carrier number. This suggests that (i) either the 3**k** structure disappears under pressure at 0.23 GPa in NpAs, 2.7 GPa in NpSb, and 3.9 GPa in NpBi; (ii) or the Fermi surface drastically changes under pressure without affecting the magnetic structure.

As it is known that in NpAs the onset of the 3**k** structure at ambient pressure is connected with a lattice expansion of $\sim$0.4%,[13] its suppression with reduced volume can be expected (0.23 GPa corresponds to $\Delta V/V_0\approx 0.3\%$). Furthermore in all pnictides of U and Np displaying a 3**k** structure, $T_{3\mathbf{k}}$ decreases under pressure.[28,17] Consequently the application of pressure weakens the interactions which are responsible for this structure. Thus, taking the resistance data alone, a magnetic phase transformation (i) is very likely.

In the following we discuss our resistance data on NpAs within a preliminary phase diagram suggested from previous

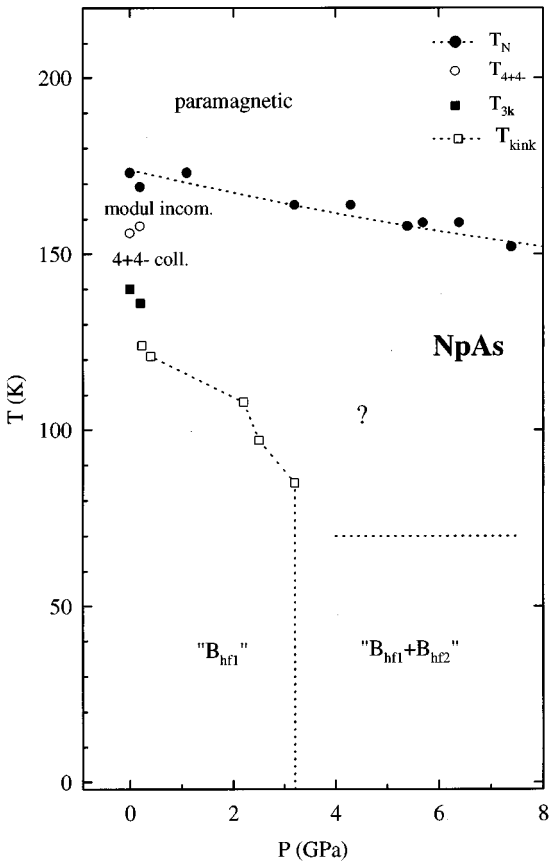

FIG. 10. NpAs: Proposed magnetic phase diagram (see also Ref. 18). The behavior at ambient pressure is well established (Ref. 4) but the volume dependence must be considered to be tentative. The Néel temperature (●) at elevated pressure is obtained from previous Mössbauer (Refs. 8 and 18) and our resistance data. The phases ''$B_{\rm hf1}$'', ''$B_{\rm hf1}+B_{\rm hf2}$'' and ''?'' denote unknown high-pressure phases. In ''$B_{\rm hf1}+B_{\rm hf2}$'' two magnetic hyperfine fields were observed. The field $B_{\rm hf2}$ is reduced by $\sim$10% relative to $B_{\rm hf1}$ (Ref. 18). It is suggested that the temperatures $T_{\rm kink}$ (□) coincide with the magnetic transition temperatures of phase ''?'' to ''$B_{\rm hf1}$.''

high-pressure Mössbauer measurements.[18,8] The pressure-induced magnetic structures in NpSb and NpBi are discussed within our results further below.

1. Magnetic phases of NpAs

The phase diagram proposed in Refs. 18 and 8 is depicted in Fig. 10 with slight modifications suggested by our resistance study. According to Refs. 18 and 8 it was shown that at low pressures up to 2.5 GPa and at 4.2 K, i.e., in the range where the resistance collapses, $B_{\rm hf}$ and e^2qQ display no significant changes. The phase denoted as ''$B_{\rm hf1}$'' in Fig. 10 was tentatively identified as the noncollinear 3**k** phase, which is already present at ambient pressure. Above 2.5 GPa the Mössbauer spectra reveal a coexistence of two magnetic hyperfine fields $B_{\rm hf1}$ and $B_{\rm hf2}$. $B_{\rm hf2}$ is reduced by $\sim$10% relative to $B_{\rm hf1}$. Note that at ambient pressure and at $T_{3\mathbf{k}} \cong 138$ K, $B_{\rm hf}$ is reduced in the collinear $4\uparrow4\downarrow$ phase by $\sim$10% relative to the 3**k** phase as well. It was suggested that in the ''$B_{\rm hf1}+B_{\rm hf2}$'' regime (see Fig. 10) the 3**k** and $4\uparrow4\downarrow$ structures coexist, since a modulated structure seems to be unlikely due to the intensities of the two fields.[8] This implies that the 3**k** phase is present at least up to 8.5 GPa in contrast to hypothesis (i). However, we emphasize that at present only the *size* of $\mu_{\rm ord}$ is known, whereas the magnetic *structure* still needs to be investigated at elevated pressure by neutron diffraction.

As described in Sec. III A the sharp rise of the resistance collapses above 0.2 GPa. Instead a kink occurs in the pressure range of 0.23–3 GPa and at temperatures below 150 K. The temperatures where the kink appears (□) are plotted in Fig. 10. The kink represents probably the transition between the ''$B_{\rm hf1}$'' phase at low-temperature and a high-temperature phase ''?'' which is unknown. This is consistent with the proposed diagram of Ref. 18. The strong hysteresis of the kink upon increasing and decreasing temperature (see Fig. 3) gives evidence for a first-order transition. Furthermore the strong hysteresis may be taken as a hint that the magnetic structure is changed above 0.23 GPa, since at ambient pressure and at 0.2 GPa the hysteresis is much smaller. The temperature of the kink (□) decreases with increasing pressure and disappears above 3 GPa, roughly in the pressure range where the second hyperfine field $B_{\rm hf2}$ occurs in the Mössbauer spectra. Consequently a transition between different magnetic phases is not visible in our resistance curves in this pressure range, as is expected from Ref. 18.

2. Pressure-induced phases in NpSb and NpBi

In NpSb the upturn is even replaced by a sharp decrease of the resistance at pressures $p \geqslant 2.7$ GPa (Fig. 4). Thus a substitution of the 3**k** phase is very likely as well. Neither the ordered moment nor e^2qQ is significantly changed in the high pressure structure which probably excludes a $4\uparrow4\downarrow$ phase.

In NpBi the upturn is still observed up to 16 GPa. It is possible that the 3**k** phase is present up to 5.3 GPa. However, we rule out its presence at higher pressures, where the crystallographic structure is tetragonal (see Sec. IV B) and is not compatible with a 3**k** magnetic order.

B. Structural transitions

High-pressure x-ray measurements at room temperature on the pnictides NpX (X=As,Sb,Bi) have revealed crystallographic phase transformations from the cubic NaCl ($B1$) to cubic CsCl ($B2$) structure in NpAs and to a distorted (tetragonal) CsCl structure in NpSb and NpBi.[19] In NpAs and NpSb the transitions are sluggish and occur in a wide pressure range, between 25–40 and 10–18 GPa, with volume compressions of 9 and 11.5 %, respectively.[29,27] In NpBi a sudden transformation appears at $\sim$8.5 GPa with a compression of 12%.[19,30] Since structural transitions can be accompanied by modifications of the Fermi surface and of magnetic properties, changes in the resistivity are expected. In the following we discuss the features observed in the resistance measurements, which can be correlated to the phase transformation.

1. Features in the resistance

In NpAs the transition pressure is possibly too high to be observed in our resistance measurement. The only striking effect is the disappearance of the logarithmic Kondo anomaly at 27.3 GPa [see Fig. 2(b)]. For NpSb, an anoma-

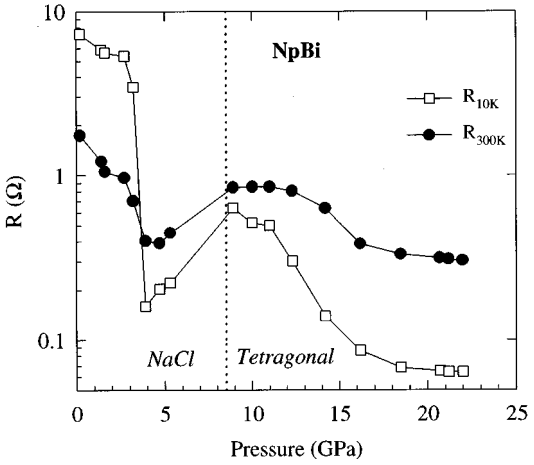

FIG. 11. NpBi: Electrical resistance measured at 10 K (□) and at 300 K (●) vs pressure. The dotted line indicates the structural transition as observed by previous high-pressure x-ray measurements (Refs. 19 and 30).

lous behavior of the resistance versus pressure curves at 4.2 K and at room temperature between 5 and 8 GPa has been attributed to the structural phase transformation.[17] The signature of magnetic order disappears in the high-pressure phase. Surprisingly the pressure range of the transition is lower than found for x-ray measurements. The different transition pressures were explained by different quasihydrostatic conditions in the high-pressure cells.[17] For NpBi the resistances at 300 and 10 K are plotted versus pressure in Fig. 11. As in NpSb, an anomaly appears in the pressure range of the structural transition (between 4 and 10 GPa). At both temperatures the resistance suddenly rises with increasing pressure. In the tetragonal phase above 10 GPa the resistance starts to decrease. The signature of magnetic order remains unchanged in the $R(T)$ curve, whereas the negative slope of T_{ord} as a function of pressure is enhanced as depicted as depicted in Fig. 7.

Since similar structural transitions appear in alkali halides (NaC→CsCl) (Ref. 31) and LaSb (NaCl→tetragonal structure, at 10 GPa with $\Delta V/V_0 \sim 10\%$),[19] they are certainly not driven by $5f$ hybridization. However, the transition may affect the $5f$ electrons. This is observed indeed in our Mössbauer study of NpSb at 9 GPa.

2. Features in the Mössbauer results of NpSb

The relative intensities ($\sim 50\%$) of the subspectra of sites 1 and 2 (see Sec. III B) suggest that at 9 GPa the $B1$ and tetragonal phase coexist with approximately the same weight. According to the resistance measurements of Ref. 17 the presence of the tetragonal phase would be expected already at 7.8 GPa which, however, is ruled out by our Mössbauer results within the experimental resolution. The distribution of magnetic hyperfine fields observed at 7.8 GPa suggests that the resistance is modified by both the structural and magnetic changes. Furthermore the different transition pressures found with different methods (6–8 GPa in the resistance, 8–9 GPa in the Mössbauer, and ~ 12 GPa in the x-ray experiment) are probably due to different quasihydrostatic conditions in the pressure cells. In the following we

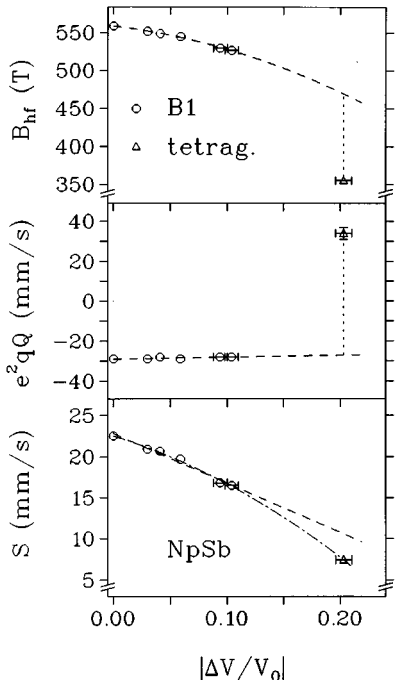

FIG. 12. NpSb: Magnetic hyperfine field B_{hf}, coupling constant of the quadrupole interaction e^2qQ, and isomer shift S relative to $NpAl_2$ plotted vs volume change. At the highest pressure (9 GPa) two crystallographic phases can be identified, NaCl phase: ○ ($|\Delta V/V_0| = 0.104$), tetragonal phase: △ ($|\Delta V/V_0| = 0.203$).

discuss the hyperfine interactions derived from the subspectrum of the tetragonal phase at 9 GPa and 4.2 K (see Figs. 9 and 12, and Table I).

Magnetic hyperfine field B_{hf2} of site 2. When extrapolating the lattice parameters of the tetragonal phase at 12 GPa (given in Ref. 27) to 9 GPa the Np-Np distance (330.6 pm) is close to the Hill limit (325 pm) and an enhanced $5f$ hybridization and crystal-field interaction can partly quench the ordered moment. Indeed we find a strong reduction of B_{hf} by $\sim 30\%$ between the $B1$ and the tetragonal phase. This corresponds to a decrease of the moment from $\sim 2.5\,\mu_B$ to $\sim 1.7\,\mu_B$. In contrast, in the $B1$ phase both hybridization and crystal-field interaction seem to play a minor role even at 9 GPa, since the ordered moment and the quadrupole coupling constant are close to the values of the Np^{3+} free-ion configuration. Therefore the effect of quenching is very small up to 9 GPa in the $B1$ phase.

Electric quadrupole interaction $(e^2qQ)_2$ of site 2. In contrast to the $B1$ phase the electric-field gradient q_2 in the tetragonal phase is certainly not induced by magnetic order. This follows from the high coupling constant $(e^2qQ)_2 \approx +34$ mm/s which is not compatible with a Np^{3+} configuration. The field gradient rather has to be attributed to the noncubic Np site symmetry in the tetragonal phase. The high value of $(e^2qQ)_2$ can be due to a distortion of the surrounding $5f$ and $6d$ cloud driven by anisotropic hybridization.

Isomer shift S_2 of site 2. The drastic drop of the isomer shift from 16.5(4) mm/s in the $B1$ phase to 7.4(4) mm/s in the tetragonal structure originates from an increase of the electron density $\rho(0)$ at the Np nucleus by $\sim 18\%$ of $\Delta\rho(0)^{Np^{3+\rightarrow 4+}}$ with $\Delta\rho(0)^{Np^{3+\rightarrow 4+}}$ being the difference of $\rho(0)$ between the Np^{3+} and Np^{4+} configurations.[26] A change

TABLE II. Volume coefficients of the magnetic ordering temperature T_{ord}, the ordered magnetic moment μ_{ord}, and of the electron density $\rho(0)$ at the nucleus. The arrow indicates the increase of $5f$ delocalization between $NpCo_2Si_2$ and $NpOs_2$.

Compound	$d\ \ln T_{ord}/-d\ \ln V$	$d\ \ln\mu_{ord}/-d\ \ln V$	$10^5\ d\ \ln\rho(0)/-d\ \ln V$	
$NpOs_2$[a]	−80.0	−46.0	+12.5	Delocalized
UN[b]	−19	−19		
$NpAl_2$[a]	−16.0	−4.0	+5.0	
NpA_s[a,c]	−1.3	−0.8	+4.2	↑
NpSb[a,c]	−3.1	−0.4	+2.8	
NpBi[c]	−0.7			
$NpGa_3$[d]	+6	−0.1	+2.6	
$NpCo_2Si_2$[a]	+7.0	+0.1	+2.4	Localized

[a]Reference 37.
[b]Reference 38.
[c]This work.
[d]Reference 39.

of $\rho(0)$ with reduced volume can be caused by a variation of the electron density at the Np site with s and $p_{1/2}$ symmetry due to the following two effects: (a) A variation of the interatomic distance (without involving the $5f$ states), e.g., by changing the overlap with the bonding orbitals of the neighbor atoms. (b) A variation of the screening of the outer s and $p_{1/2}$ electrons by the $5f$ charge cloud, e.g., if the $5f$ states hybridize.

The value of S_2 does not give a clear evidence in favor or against $5f$ delocalization, since besides the *volume* the *crystallographic structure* changes. With decreasing volume of the unit cell the overlap of the neighbor orbitals and consequently $\rho(0)$ is expected to increase as long as the crystal structure remains unchanged. This is observed in NpSb in the $B1$ phase up to 9 GPa. However, it has been shown previously that a pressure-induced phase transformation accompanied by a volume collapse can lead to a decrease of $\rho(0)$, if the nearest-neighbor distance increases (e.g., in ZnO).[32] As in NpSb at the *structural* transition the nearest-neighbor distance $d_{Np\text{-}Sb}$ increases by $\sim 4\%$,[27] it is possible that mechanism (a) can contribute to a decrease or at least a smaller increase of $\rho(0)$ than would be expected from the *volume* change alone.

Effect (b) has been suggested to be important for some actinide intermetallics,[33,34] since $5f$ delocalization leads to a loss of $5f$ spectral density in real space, i.e., the $5f$ wave functions are more extended outside of the core region.[35] This leads to a reduction of μ_{ord} or B_{hf}, and tends to enhance $\rho(0)$. Due to the strongly reduced magnetic hyperfine field B_{hf} we can expect that strong $5f$ hybridization in the tetragonal phase raises $\rho(0)$.

A comparison of the isomer shift versus volume curve as depicted in Fig. 12 with that of $EuAl_2$ (Ref. 36) shows that both systems display a similar increase and curvature of $\rho(0)$, if the change of the isomer shift as a function of volume is calculated relative to the difference of the two charge states Np^{3+}, Np^{4+} and Eu^{2+}, Eu^{3+} respectively. In $EuAl_2$ no phase transformation appears and the $4f$ electrons remain in a localized Eu^{2+} configuration up to 50 GPa. Therefore f screening effects can be neglected and the increase of $\rho(0)$ is mainly caused by an enhanced overlap of the neighbor orbitals with reduced *volume*. For NpSb we rather suggest that a change of the overlap due to the *structural* transition (a) and an increase of $\rho(0)$ due to $5f$ delocalization (b) partly compensate and that both effects play a major role.

C. Magnetic behavior under pressure

According to previous Mössbauer results performed on NpAs up to 8.5 GPa, small $5f$ delocalization was suggested due to the decrease of the Néel temperature, the ordered moment and the induced quadrupole interaction with reduced volume.[18] The question arises whether magnetism is suppressed at higher pressures. Furthermore, from the previous resistance study on NpSb it was proposed that magnetic order disappears above ~ 8 GPa.[17]

Our resistance data on NpAs give evidence that magnetism is present at least up to ~ 16 GPa (see Sec. III A). In NpSb, the Mössbauer data obtained at 9 GPa clearly reveal the presence of magnetic order in the NaCl and in the tetragonal structure (see Figs. 9 and 12, and Sec. IV B). In NpBi, the signature of magnetism in the resistance behavior is present up to ~ 16 GPa.

The systematics of the magnetic behavior under pressure can be extracted from Table II, where the volume coefficients $d\ln\mu_{ord}/-d\ \ln V$, $d\ \ln T_{ord}/-d\ \ln V$, and $d\ \ln\rho(0)/-d\ \ln V$ are listed for the Np pnictides and other Np-based compounds. These volume dependencies allow the classification of a given system in terms of $5f$ delocalization.[40] UN (Ref. 38) and $NpOs_2$ (Ref. 18) are typical representatives of itinerant $5f$ systems whereas $NpCo_2Si_2$ is classified as localized.[18] The ordering temperature and the ordered moment of UN and $NpOs_2$ strongly decrease under pressure as shown from the negative values of $d\ \ln T_{ord}/-d\ \ln V$ and $d\ \ln\mu_{ord}/-d\ \ln V$. Furthermore, in $NpOs_2$ the μ_{ord} versus volume curve displays a strong negative curvature.[18] In $NpOs_2$ the high value of the coefficient of the electron density $\rho(0)$ at the Np nucleus $d\ \ln\rho(0)/-d\ \ln V$ is characteristic of a strong $5f$ delocalization.[37] Furthermore μ_{ord} is considerably reduced relative to the free-ion value already at ambient pressure. In contrast, in the localized system $NpCo_2Si_2$ $\rho(0)$ and μ_{ord} exhibit a small variation and T_{ord} increases with reduced volume (Table II).

Due to the high values of μ_{ord} and T_N at ambient pressure and the comparatively small values of the volume coefficients (see Table II) the behavior of the pnictides NpX is in contrast to what is expected from a $5f$ band model.

Furthermore it is unlikely that μ_{ord} and T_N are reduced by Kondo interaction at elevated pressure. In this case an increase of the slope of the logarithmic resistance anomaly would be expected under pressure.[41] In contrast, in NpSb and NpBi the slope decreases under pressure and the anomaly disappears above 2.7 GPa and 3 GPa, respectively. In NpAs the slope is nearly constant, i.e., shows no increase and disappears above 25 GPa.

For the pnictides of Np we rather suggest a model, in which the exchange between the magnetic moments is mediated by the conduction electrons through RKKY interaction. The parameters which usually enter into a calculation of the ordering temperature are the exchange integral J_{5f-c} between the localized f shells and the conduction electrons, the magnetic moment μ, and the conduction band susceptibility χ. According to de Gennes,[42] in a mean-field approximation T_{ord} scales with

$$T_{\text{ord}} \propto \chi J_{5f-c}^2 \mu(\mu+1). \tag{1}$$

First we discuss if the variation of J_{5f-c} and μ with reduced volume can explain the decrease of T_N in NpX neglecting the volume dependence of χ. The exchange integral J_{5f-c} is expected to increase under pressure,[35,43] which strengthens the indirect coupling between the $5f$ moments according to Eq. (1) and raises T_{ord}. At the same time pressure enhances $5f$ delocalization and reduces μ, which weakens magnetic order. For example this competition was invoked to explain the pressure behaviour of UTe, where T_{ord} increases at low pressures, shows a maximum at 7.5 GPa and decreases at higher pressures.[35,44] This example demonstrates that T_{ord} is decreased if the $5f$ delocalization is strong enough. If we assume a dominant $5f-p$ mixing in NpX (Ref. 9) J_{5f-c} scales with $J_{5f-c} \propto 1/V^{10/3}$.[39] To overcompensate the increase of J_{5f-c}, μ would have to decrease with a much higher power of the volume than observed in NpAs and NpSb in order to match the linear decrease of T_{ord} (see Fig. 13 and Ref. 8). This suggests that a small $5f$ delocalization cannot be the major mechanism which reduces T_N in NpX.

A phenomenological comparison gives further evidence. If we assume that in NpX and USb,[28] the decrease of T_N is driven by $5f$ delocalization, a stronger delocalization would be expected than in UTe or UAs, where T_{ord} rises. Furthermore, in NpSb the $5f$ states should be more effectively delocalized than in NpAs, due to their higher volume coefficient $d\ \ln T_{\text{ord}}/d\ \ln V$ (see Table II). However, in a simple picture, an increase of $5f$ localization is expected between U and Np compounds, e.g., UAs→NpAs and along the series NpAs→NpSb→NpBi or UAs→USb, i.e., with increasing radius of the ligand atom in group V of the Periodic Table.[45] A comparison of the series NpAs→NpSb→NpBi in Table II shows that the volume dependence of the ordered moment (magnetic hyperfine field) is probably a more reliable parameter for the degree of $5f$ delocalization than T_{ord}. The ordered moment shows a weaker variation in NpSb than in NpAs, in agreement with the simple picture of $5f$ delocalization in NpX given above. Furthermore, in NpSb the quadrupole coupling constant is nearly constant between ambient pressure and 9 GPa in the $B1$ phase giving no evidence for $5f$ delocalization. In contrast, in NpAs $|e^2\mathbf{q}Q|$ is reduced at 8.5 GPa by $\sim 20\%$.[8] A comparison of the derivatives of $\rho(0)$ suggests as well a stronger degree of $5f$ delocalization in NpAs than in NpSb.

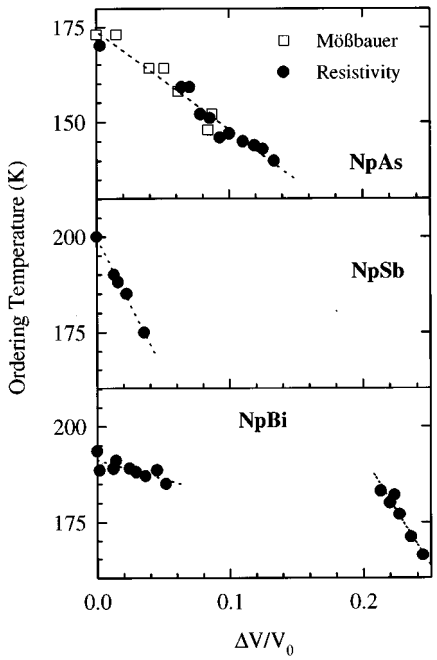

FIG. 13. Néel temperatures T_N obtained from our resistance data (●) for NpAs, NpSb (Ref. 17), and NpBi and from Mössbauer data (□) for NpAs (Refs. 8 and 18) plotted vs volume change.

Although the decrease of the ordered moment actually indicates a small $5f$ delocalization in NpX, the decrease of T_N under pressure is more likely due to a reduction of the band susceptibility χ. This seems surprising, since the decrease of the resistances under pressure (see Figs. 1–5) is probably caused by an enhancement of the carrier density. For a free-electron gas χ scales with the latter. Therefore in this model χ is expected to rise with pressure. However, we rather suggest that χ is *weakened* by a pressure induced change of the Fermi surface.

In a more realistic model the band susceptibility $\chi(\mathbf{q})$ as a function of the reciprocal vector $\mathbf{q}$ may be approximated by[46]

$$\chi(\mathbf{q}) \propto \sum_{nn'\mathbf{k}} \frac{f_{n\mathbf{k}} - f_{n'\mathbf{k}-\mathbf{q}}}{\varepsilon_{n'}(\mathbf{k}-\mathbf{q}) - \varepsilon_n(\mathbf{k})}, \tag{2}$$

where $f_{n\mathbf{k}}$ is the Fermi-Dirac function and $\varepsilon_n(\mathbf{k})$ the energy of the band n at the reciprocal vector $\mathbf{k}$. It follows from Eq. (2) that $\chi(q)$ can diverge at certain $\mathbf{q}$ vectors. The resulting peaks can be produced for example by the parallel or nesting regions at the Fermi surface.[46] This effect was made responsible for the magnetic behavior of several metallic systems, e.g., heavy rare-earth metals[46] and Cr.[47] The presence of nesting regions was indeed assumed for NpAs from theoretical considerations to explain the band gaps appearing at the onset of the $3\mathbf{k}$ structure (see Sec. IV A). It is consistent to assume that nesting and its reduction under pressure cause several effects observed in our experiments: The decrease of

T_{ord} can be due to a decrease of the peaks of $\chi(\mathbf{q})$ at certain $\mathbf{q}$ vectors (2). The suppression of nesting may also explain the disappearance of the band gaps at elevated pressure, which results in the resistance collapse discussed in Sec. IV A. Furthermore, a pressure-induced modification of $\chi(q)$ can be responsible for changes of the magnetic structures which are very sensitive to $\chi(q)$.

V. CONCLUSIONS

Our data were discussed under three important aspects: the changes of the magnetic phases, particularly the 3**k** phase, the influence of the structural transition on $5f$ delocalization, and the magnetic behavior in terms of $5f$ delocalization in the low-pressure NaCl phase.

The disappearance of the sharp upturn and the collapse of the resistance above 0.23 GPa (NpAs) and 2.7 GPa (NpSb) in the temperature range of the 3**k** structure at ambient pressure indicates that the 3**k** phase is replaced by another magnetic structure. Previous Mössbauer measurements on NpAs and our new results on NpSb demonstrate that μ_{ord} shows no significant reduction in the magnetic phases at high pressures. These phases are consequently not identical with the collinear $(4\uparrow 4\downarrow)$ structure, which displays a smaller moment. An investigation of these phases calls for a neutron-diffraction measurement under pressure, which in the case of NpAs is at present technically feasible due to its low transition pressure. This is of urgent importance since to our knowledge all pressure investigations carried out so far on actinide systems displaying a 3**k** structure, seem to suggest that the 3**k** regime is weakened or even suppressed with reduced volume.[28,48] Furthermore, high-pressure neutron investigations on CeP and CeAs, where the upturn of $\rho(T)$ disappears as well,[49] may examine if the 3**k** structure disappears also in these systems. If this is the case the question arises whether this is a general rule for a certain group of f systems.

At the structural transformation of NpSb from the NaCl to the tetragonal phase driven by external pressure, magnetism is still present in the tetragonal regime. However, the strongly reduced magnetic hyperfine field indicates an enhanced $5f$ delocalization. This can neither be confirmed nor disproved by the behavior of the isomer shift, since several contributions are expected and can partly compensate. The role which $5f$ delocalization really plays can be examined by theory, e.g., with a similar approach as recently applied to UTe to explain effects of $5f$ hybridization on magnetism.[35] An understanding of the isomer shift demands fully relativistic band-structure calculations, similar in type as applied to ZnO.[32]

We suggest that the pressure-induced decrease of the Néel temperature in the pnictides of Np is due to a Fermi surface effect besides a small $5f$ delocalization. This can be examined by a calculation of the band susceptibility $\chi(\mathbf{q})$ as a function of volume reduction. Our results for NpAs and NpBi give evidence that magnetic order persists at least up to 16 GPa. The disappearance of the Kondo anomaly of the resistance in the paramagnetic range has also been found in other systems of the light actinides, e.g., $NpGa_3$ (Ref. 39) and UTe.[44] The origin of this effect also remains to be investigated by theory. In Ref. 9 a model of a magnetic polaron liquid state has been suggested to explain the presence of the anomaly in some pnictides where the carrier density is remarkably low due to their semimetallic state. In our case, at elevated pressure the anomaly disappears although our resistance data indicate an increase of the carrier density.

ACKNOWLEDGMENTS

It is a pleasure to thank M. S. S. Brooks, J. P. Sanchez, and G. H. Lander for stimulating discussions. The high-purity Np metal required for the fabrication of NpAs, NpSb, and NpBi was made available in the framework of a collaboration with the Lawrence Livermore and Los Alamos National Laboratories and the U.S. Department of Energy. Support given to V.I. and S.Z. by CEC is also acknowledged.

[1] B. Coqblin and J. R. Schrieffer, Phys. Rev. **185**, 847 (1969).
[2] S. H. Liu, in *Handbook of the Physics and Chemistry of Rare Earths*, edited by K. A. Gschneidner, L. Eyring, G. H. Lander, and G. R. Choppin (North-Holland, Amsterdam, 1993), Vol. 17, Chap. 111, pp. 95–97.
[3] J. M. Fournier and E. Gratz, in *Handbook of the Physics and Chemistry of Rare Earths* (Ref. 2), Vol. 17, Chap. 115, pp. 512–514.
[4] P. Burlet, D. Bonnisseau, S. Quezel, J. Rossat-Mignod, J. C. Spirlet, J. Rebizant, and O. Vogt, J. Magn. Magn. Mater. **63&64**, 151 (1987).
[5] P. Burlet, F. Bourdarot, J. Rossat-Mignod, J. P. Sanchez, J. C. Spirlet, J. Rebizant, and O. Vogt, Physica B **180&181**, 131 (1992).
[6] J. P. Sanchez, P. Burlet, S. Quézel, D. Bonnisseau, J. Rossat-Mignod, J. C. Spirlet, J. Rebizant, and O. Vogt, Solid State Commun. **67**, 999 (1988).
[7] M. N. Bouillet, Ph.D. thesis, Université Joseph Fourier Grenoble, 1993.
[8] U. Potzel, Ph.D. thesis, Technische Universität München, 1987.
[9] T. Kasuya, J. Alloys Compd. **223**, 251 (1995).
[10] M. Amanowicz, Ph.D. thesis, Université de Grenoble, 1995.
[11] E. Pleska, Ph.D. thesis, Université Joseph Fourier Grenoble, 1990.
[12] G. H. Lander and P. Burlet, Physica B **215**, 7 (1995).
[13] A. T. Aldred, B. D. Dunlap, A. R. Harvey, D. J. Lam, G. H. Lander, and M. H. Mueller, Phys. Rev. B **9**, 3766 (1974).
[14] Y. S. Kwon, Y. Haga, O. Nakamura, T. Suzuki, and T. Kasuya, Physica B **171**, 324 (1991).
[15] T. Suzuki, Y. S. Kwon, S. Ozeki, Y. Haga, and T. Kasuya, J. Magn. Magn. Mater. **90&91**, 493 (1990).
[16] J. Schoenes, B. Frick, and O. Vogt, Phys. Rev. B **30**, 6578 (1984).
[17] M. Amanowicz, D. Braithwaite, V. Ichas, U. Benedict, J. Rebizant, and J. C. Spirlet, Phys. Rev. B **50**, 6577 (1994).
[18] W. Potzel, G. M. Kalvius, and J. Gal, in *Handbook of the Physics and Chemistry of Rare Earths* (Ref. 2), Vol. 17, Chap. 116, pp. 582–584.
[19] U. Benedict and W. B. Holzapfel, in *Handbook of the Physics*

and Chemistry of Rare Earths (Ref. 2), Vol. 17, Chap. 113, pp. 276–280.
[20] J. C. Spirlet and O. Vogt, in *Handbook on the Physics and Chemistry of the Actinides*, edited by A. J. Freemann and G. H. Lander (Elsevier, Amsterdam, 1984), p. 79.
[21] B. Bireckoven and J. Wittig, J. Phys. E **21**, 841 (1988).
[22] W. Potzel, G. M. Kalvius, and J. Gal, in *Handbook of the Physics and Chemistry of Rare Earths* (Ref. 2), Vol. 17, Chap. 116, p. 570.
[23] A. Seret (private communication).
[24] M. A. Il'ina and E. S. Itskevich, JETP Lett. **11**, 218 (1970).
[25] T. Gouder (private communication).
[26] W. Potzel, G. M. Kalvius, and J. Gal, in *Handbook of the Physics and Chemistry of Rare Earths* (Ref. 2), Vol. 17, Chap. 116, p. 563.
[27] S. Dabos-Seignon, U. Benedict, S. Heathman, and J. C. Spirlet, J. Less-Common Met. **160**, 35 (1990).
[28] D. Braithwaite, I. N. Goncharenko, J.-M. Mignot, A. Ochiai, and O. Vogt, Europhys. Lett. **35**, 121 (1996).
[29] S. Dabos, C. Dufour, U. Benedict, S. Heathman, and J. C. Spirlet, J. Less-Common Met. **160**, 52 (1990).
[30] M. Gensini, Ph.D. thesis, Université de Liège, 1992.
[31] J. A. Majewski and P. Vogl, Phys. Rev. Lett. **57**, 1366 (1986); Phys. Rev. B **35**, 9666 (1987); Acta Phys. Pol. A **73**, 341 (1988).
[32] H. Karzel, W. Potzel, M. Köfferlein, W. Schiessl, M. Steiner, U. Hiller, G. M. Kalvius, D. W. Mitchel, T. P. Das, P. Blaha, K. Schwarz, and M. P. Pasternak, Phys. Rev. B **53**, 11 425 (1996).
[33] J. Gal, I. Yaar, S. Fredo, I. Halevy, W. Potzel, S. Zwirner, and G. M. Kalvius, Phys. Rev. B **46**, 5351 (1992).
[34] S. Zwirner, W. Potzel, J. C. Spirlet, J. Rebizant, J. Gal, and G. M. Kalvius, Physica B **190**, 107 (1993).
[35] B. R. Cooper, Q. G. Sheng, U. Benedict, and P. Link, J. Alloys Compd. **213/214**, 120 (1994).
[36] A. Gleissner, W. Potzel, J. Moser, and G. M. Kalvius, Phys. Rev. Lett. **70**, 2032 (1993).
[37] W. Potzel, G. M. Kalvius, and J. Gal, in *Handbook of the Physics and Chemistry of Rare Earths* (Ref. 2), Vol. 17, Chap. 116, pp. 589–592.
[38] J. M. Fournier, J. Beille, A. Boeuf, C. Vettier, and A. Wedgwood, Physica B **102**, 282 (1980).
[39] S. Zwirner, V. Ichas, D. Braithwaite, J. C. Waerenborgh, S. Heathman, W. Potzel, G. M. Kalvius, J. C. Spirlet, and J. Rebizant, Phys. Rev. B **54**, 12 283 (1996).
[40] J. M. Fournier, Physica B **130**, 268 (1985).
[41] A. Eiling and J. S. Shilling, Phys. Rev. Lett. **46**, 364 (1981).
[42] P. G. de Gennes, J. Phys. Radium **23**, 510 (1962).
[43] T. Gasche, Ph.D. thesis, Uppsala University, 1994.
[44] P. Link, U. Benedict, J. Wittig, and H. Wühl, J. Phys.: Condens. Matter **4**, 5585 (1992).
[45] D. D. Koelling, B. D. Dunlap, and G. W. Crabtree, Phys. Rev. B **31**, 4966 (1985).
[46] J. Jensen and A. R. Mackintosh, *Rare Earth Magnetism* (Oxford Science, Oxford, 1991), pp. 32–33 and 47–50.
[47] W. M. Lomer, Proc. Phys. Soc. London **80**, 489 (1962).
[48] J.-M. Mignot, I. N. Goncharenko, D. Braithwaite, and O. Vogt, J. Phys. Soc. Jpn. **65**, 91 (1996).
[49] Y. Okayama, H. Takahashi, N. Mori, Y. S. Kwon, Y. Haga, and T. Suzuki, J. Magn. Magn. Mater. **108**, 113 (1992).